Journal-Ref: Astronomy Letters, 2013, Vol. 39, No. 1, pp. 26-37

Asymmetric Illumination of a Circumbinary Disk in the Presence of a Low-Mass Companion

©2012 г. **T. Demidova**[1*], **V. Grinin**[1,2], **N. Sotnikova**[1,2]

1 - Pulkovo Astronomical Observatory, Russian Academy of Sciences,
Pulkovskoe shosse 65, St. Petersburg, 196140 Russia,
2 - Sobolev Astronomical Institute, St. Petersburg State University,
Universitetskii pr. 28, St. Petersburg, 198504 Russia,

Received May 18, 2012

Abstract

The model of an young star with a protoplanetary disk and a low-mass companion ($q \leq 0.1$), which is moving on a circular orbit, inclined to the disk plane, is considered. The hydrodynamic models of such a system were calculated by SPH method. It was shown the distortions in the disk, caused by the orbital motion of the companion, lead to the strong dependence of illumination conditions of the disk on the azimuth (because of extinction between the star and the disk surface) and, therefore, it leads to the appearance of large-scale asymmetry in images of disks. The calculations showed the dependence of the illumination on the azimuth was stronger in the central part of the disk than on the periphery. Bright and dark domains are located not symmetry with respect to the line of nodes. The sizes and locations of the domains are depended on the model parameters as well as on the phase of the orbital period. The bright and dark domains do not follow the companion, but they make small amplitude oscillations with respect to some direction. The properties of the model, which were written above, open new opportunities of searching low-mass companions in the vicinity of young stars. The stars with protoplanetary disks, which are observed face-on or under the small inclination angle i, are the best ones for this purpose.

Key words: *protoplanetary disks, hydrodynamics, low-mass companions, noncoplanar orbits.*

*e-mail: proxima1@list.ru

INTRODUCTION

Many young stars are known to be surrounded by circumstellar gas-dust disks radiating in the infrared (IR) and submillimeter wavelength ranges (see, e.g., the review by Natta et al. (2000)). In the overwhelming majority of cases, observations provide only information about the integrated (i.e., from the entire disk) IR radiation (Mendoza 1966; Cohen 1975). In the visual spectral range, the circumstellar disks radiate very little, mainly through the scattered radiation of their central stars[1].Nevertheless, most of the circumstellar disk images known to date have been obtained precisely in the optical spectral range with the Hubble Space Telescope by the method of coronagraphy (McCaughrean and O'Dell 1996; McCaughrean et al. 2000; Grady et al. 2000; Krist et al. 2000; Clampin et al. 2003; and others). Among them, there are disks seen edge-on or at a small angle to the line of sight (Burrows et al. 1995; McCaughrean and O'Dell 1996; Stapelfeldt et al. 1998; and others) and disks seen nearly face-on (Grady et al. 2000; Krist et al. 2000; and others). Many of the disks have an asymmetric shape that is often explained by anisotropic scattering of stellar radiation by circumstellar dust grains. This mechanism is efficient in the cases where the disk is inclined to the plane of the sky.

However, the nature of the asymmetry in circumstellar disk images is not exhausted by this mechanism alone. The asymmetry of the disk surface brightness can also be caused by an anisotropic illumination of the disk by the central star, for example, due to the presence of spots on the star. This model was considered by Wood and Whitney (1998) in connection with the detection of variability in the image of HH30's protoplanetary disk by Burrows et al. (1996). It is quite real, because the rotational modulation of the brightness of young stars due to a nonuniform surface brightness is a well-known observational fact (see, e.g., Vrba et al. 1986).

Another cause of the anisotropic disk illumination can be the absorption of stellar radiation by circumstellar matter if it is distributed nonuniformly in azimuth. Hydrodynamic calculations show (Artymowicz and Lubow 1996; Larwood and Papaloizou 1997; Sotnikova and Grining 2007; Hanawa et al. 2010; Kaigorodov et al. 2010) that such conditions can arise in young binary systems accreting matter from the remnants of a protostellar cloud (below referred to as a CB (circumbinary) disk). Under the action of periodic perturbations induced by the orbital motion of the companion, spiral density waves and gas flows propagating into the system's inner regions are formed in the CB disk. If such a system is observed at a small angle to the disk plane, then, as our calculations showed (Sotnikova and Grinin 2007; Demidova et al. 2010a, 2010b; Grinin et al. 2010), the motion of large-scale structures in it can cause great circumstellar extinction variations and, as a consequence, a large-amplitude brightness modulation of the system. It turned out than a noticeable (in amplitude) photometric effect could be caused by the orbital motion of a low-mass companion or a protoplanet (Demidova et al. 2010b) and that this effect is enhanced if the companion's orbit is inclined to the disk plane (Grinin et al. 2010).

It should be noted that the situation where the orbit of the companion (planet) does not coincide with the midplane of the common disk or the equatorial plane of the central star is not something exceptional. This can result from a nonaxisymmetric distribution of specific angular momentum in the protostellar cloud from which the star and protoplanetary disk are born. A star whose rotation axis may not coincide with the rotation axis of the protoplanetary disk is formed during the gravitational contraction of such a cloud. This possibility has been discussed in recent years (see, e.g., Bate et al. 2010) in connection with the unexpected results of spectroscopic observations of stars with exoplanets during the transit of a planet over the stellar disk. They showed that the orbital planes of several exoplanets do not coincide with the equatorial plane of the stars (Hébrard et al. 2009; Winn et al. 2009a, 2009b; Pont et al. 2010; Narita et al. 2011; Brown et al. 2012). Previously, Burrows et al. (1995) found that the inner part of the circumstellar disk around β Pic Pic is inclined by several degrees to its outer part and hypothesized that this inclination was caused by the motion of a planet whose orbit is also inclined to the disk plane. The corresponding model was developed by Mouillet et al. (1997) and Larwood and Papaloizou (1997), and the planet itself has also been discovered recently (Lagrange et al. 2009; Chauvin et al. 2012). The same picture is observed for the Herbig Ae star CQ Tau: the inner part of its circumstellar disk is inclined approximately by 30° to the disk periphery (Eisner et al. 2004; Chapillon et al. 2008).

In this paper, we investigate the influence of hydrodynamic perturbations in such systems on the extinction variations between the central star and disk surface. The goal of our calculations is to determine the disk illumination conditions at various distances from the center and its dependence on azimuth.

[1]UX Ori stars at eclipses (Grinin et al. 1991) and young objects with edge-on circumstellar disks constitute an exception.

THE METHOD OF CALCULATIONS

We consider the model of a binary system that consists of a central star and a low-mass companion ($q = m_2 : m_1 \leq 0.1$), moving in a circular orbit of radius a. The orbital plane is assumed to be inclined to the CB disk midplane. The mass of the star is taken to be $2\,M_\odot$ this value roughly corresponds to the mass of a typical Herbig Ae star); the orbital period of the companion is 1 year.

As in our previous papers, the 3D hydrodynamic calculations were performed by the SPH (Smoothed Particle Hydrodynamics) method in the isothermal approximation. The implementation of this method is described in detail in Sotnikova (1996). One of the main hydrodynamic parameters, the effective viscosity of the disk, was determined via the dimensionless speed of sound c, expressed in fractions of the Keplerian velocity in the companion's orbit. This parameter was varied within the range $c = 0.001 - 0.08$. The parameters of the problem also include the mass accretion rate onto the binary components $\dot{M}_a$ and the opacity κ, per gram of circumstellar matter (as in our previous papers, κ was taken to be 250 cm^2/g (Natta and Whitney 2000), which corresponds to the optical properties of the circumstellar dust in young circumstellar disks in the visual spectral range). The dust-to-gas mass ratio was taken to be the same as that, on average, in the interstellar medium, 1 : 100.

The calculations were performed using from 60000 to 2×10^5 test particles in a region of radius $10\,a$. Our calculations showed that after 30 rotations the system finishes the relaxation stage (with the formation of a central gap) and the distribution of SPH particles reflects best the behavior of the matter in the CB disk. The disk model calculated in this way was smoothed over the cells of a 3D mesh (with a step of $0.1\,a$). This procedure allowed the influence of random fluctuations in the distribution of SPH particles to be reduced while retaining all details of the flow structure.

As an example, Fig. 1 shows the distribution of SPH particles in one of the calculated models (before the smoothing procedure described above). We see that the deviations from azimuthal symmetry are greatest near the inner boundary of the CB disk (the disk is puffed up). At distances of the order of five orbital radii, the distribution of matter in the CB disk is already azimuthally symmetric, and such a disk differs little in structure from the disk around a single star of the same mass. To investigate the influence of density waves and nonuniform structure of the inner region of the CB disk on the illumination of its outer layers, the model distribution of particles was smoothly extended to distances of $50\,a$ by using the standard model of a flared disk:

$$h(r) = h_0\Big(\frac{r}{r_0}\Big)^\beta, \qquad (1)$$

where $2\,h(r)$ — is the geometrical thickness of the disk at distance r from the symmetry axis, the parameter $\beta = 5/4$ (Kenyon and Hartmann 1987), and the initial values of $h_0 = a$, and the radius $r_0 = 5a$.

Calculation of the Disk Illumination

We calculated the disk surface illumination from the formula

$$F(r,\phi) = \frac{L_* e^{-\tau(r,\phi)}}{4\pi(r^2+h^2)}\sin\gamma, \qquad (2)$$

where L_* — is the luminosity of the central star, $\tau(r,\phi)$ — is the optical depth of the dust layer between the star and an arbitrary point on the disk at distance r from the symmetry axis and azimuth ϕ, γ — is the angle between the vector connecting the star and the point on the disk surface and the tangent to the disk surface at this point (for details, see Tambovtseva et al. 2006).

When calculating $\tau(r,\phi)$ we used the same method as in our previous papers (see, e.g.,Demidova et al. 2010a): having compared the accretion rate of test particles onto the binary components with the accretion rate specified as a parameter of the problem (in the range $\dot{M}_a = 10^{-9} - 10^{-11} M_\odot yr^{-1}$), we determine the test particle mass m_d. Then, $\tau(r,\phi) = m_d \cdot n(r,\phi)\cdot k/S$, where $n(r,\phi)$ is the number density of test particles in the column between the star and a point on the disk surface with coordinates r и ϕ, S is the cross section of this column.

Allowance for the Scattered Radiation

The direct stellar radiation is the main disk surface illumination source. This radiation does not penetrate into the shadow zone because of strong absorption on the way, in the perturbed disk region, and it is illuminated only by the radiation scattered by circumstellar dust. To estimate the contribution from this radiation, we calculated the intensity of the scattered radiation for several models in the single-scattering approximation. This approximation is applied in the cases (see, e.g., Tambovtseva et al. 2006) where the single-scattering albedo differs noticeably from unity, because under these conditions the role of multiple scatterings is minor.

Below, we used the same scheme of calculations as in the above paper (Tambovtseva et al. 2006): the inner CB disk region ($r < 5a$) was divided into, cells, each being considered as a scattering element with density $\rho_i = m_d \cdot n_i$, where n_i s the number of

particles in the ith cell. For each surface element of the CB disk, the scattered light was calculated as the sum of the fluxes scattered by each cell toward the chosen disk surface element. We took into account the absorption of radiation by dust both on the way from the star to the scattering volume and on the way from it to the illuminated disk surface element:

$$F_{sc}(r,\phi) = k_{sc}\sum_i \frac{L_*}{4\pi d_1^2}\frac{\rho_i}{4\pi d_2^2} f(\theta_i) e^{-\tau_i}\cos\xi_i. \quad (3)$$

Here, d_1 is the distance from the primary component to the scattering cell, d_2 is the distance from the scattering cell to the unit CB disk surface element illuminated by the scattered radiation, k_{sc} is the scattering coefficient, $\tau_i = \tau_1 + \tau_2$ is the sum of the optical depths of dust on the way from the primary component to the scattering cell (τ_1) and from the scattering cell to the surface element on the outer CB disk (τ_2), ξ_i is the angle between the direction of the scattered radiation from the center of the scattering cell to the surface element on the CB disk under consideration and the normal to the disk surface at this point. In our calculations, we used the Henyey-Greenstein phase function:

$$f(\theta) = \frac{1}{4\pi}\frac{1-g^2}{(1+g^2-2g\cos\theta)^{3/2}}, \quad (4)$$

where θ is the scattering angle, g is the asymmetry factor (taken to be 0.5). The single-scattering albedo was taken to be 0.4, which roughly corresponds to the optical properties of circumstellar dust in the V band (Natta and Whitney 2000). Taking this into account, the scattering coefficient is $k_{sc} = 100\mathrm{cm}^2/\mathrm{g}$.

RESULTS

We calculated the disk surface illumination by the method described above for several models. The input model parameters are the orbital inclination to the disk plane α, the component mass ratio q, and the disk viscosity parameter c. Figure 2 presents the results of our calculations for two models differing by the orbital inclination: $\alpha = 10^\circ$ and $\alpha = 30^\circ$. We see that, in both cases, the disk illumination is highly nonuniform in azimuth due to the absorption of the direct stellar radiation in the perturbed region (near the inner disk boundary). The degree of deformation of the inner CB disk increases with α causing the area of the shadow from it on the disk to increase. A nontrivial peculiarity in the disk brightness distribution attributable to the distribution of matter in the perturbed CB disk region is that the *line separating the bright and dark regions on the disk does not coincide with the line of nodes*. For quantitative estimations, we determined the location of this line in such a way that the ratio of the integrated illuminations of the disk regions on different sides of this line was maximal. Our calculations showed that the inclination of this line to the line of nodes changes with model parameters within a comparatively narrow range: $\phi_l \approx 50-70^\circ$. In particular, in the models with $\alpha = 10^\circ$ the angle $\phi_l = 57^\circ$, with $\alpha = 30^\circ$ — $\phi_l = 59^\circ$ (Fig. 2).

As can be seen from Fig. 3, the location of the shadow zone relative to the line of nodes in the models considered is almost independent of the companion's orbital inclination. The illumination minimum is reached in a region with an azimuthal angle $\phi_{sh} \approx 330^\circ$. Since the minimum illumination is due to the maximum absorption of radiation in the perturbed disk region, the result obtained suggests that the region of maximum disk deformation does not coincide with the region in which the companion rises to the maximum height above the CB disk plane ($\phi = 270^\circ$). Such a distribution of matter in the inner disk stems from the fact that the secondary component entrains part of the matter once it has passed the point of greatest distance from the CB disk plane, which causes the CB disk thickness in this direction to increase. Other things being equal, the larger the viscosity, the higher the efficiency of this process (see below).

The deformation of the inner CB disk region also depends on the companion's mass. The greater the value of q, the larger the amplitude of the perturbations in the disk and the stronger the asymmetry in its illumination. In this case, the position of the illumination minimum still corresponds to $\phi_{sh} \approx 330^\circ$ (Fig. 4).

Viscosity affects the illumination conditions in the following way: the CB disk becomes denser and thinner with decreasing viscosity. As a result, the area of the shadow on the disk is reduced. For example, in the models with a "cold" disk ($c \le 0.03$) the disk is illuminated uniformly already at $R \ge 20a$, while in the models with c $c = 0.05$ (at the same value of q) the shadow zone extends to $R = 30a$. The location of the line separating the bright and dark regions on the disk also depends on viscosity and varies within the range $\phi_l = 50-65^\circ$. In addition, the azimuthal angle of the illumination minimum in the shadow zone increases with viscosity (Fig. 5). This suggests that the disk matter is entrained more actively by the secondary component during its orbital motion and shields the star more strongly with increasing viscosity.

Figures 6 and 7 show the two limiting situations considered in our calculations where a noticeable asymmetry in the CB disk illumination is still possible: the model with a small orbital inclination to the disk plane ($\alpha = 3^\circ$) and the model in which the mass of the perturbing body is of the order of several Jupiter

masses ($q = 0.003$). Under these conditions, the perturbations in the disk induced by the companion's orbital motion are small. Nevertheless, as can be seen from Figs. 6 and 7, an asymmetry in the disk illumination due to an asymmetric distribution of absorbing matter is clearly seen in the central disk region in these cases as well. Our calculations showed that the degree of asymmetry in the disk illumination is more sensitive to variations in α, than to variations in the companion's mass. Therefore, even a planet with a mass of several Jupiter masses can produce a noticeable asymmetry in the protoplanetary disk illumination if its orbit has an appreciable inclination to the disk plane ($\alpha \geq 10^\circ$).

Influence of the Scattered Light

In addition to the direct radiation, the disk surface is also illuminated by the scattered light. The contribution from this radiation on the bright (illuminated) part of the disk is negligible compared to the direct stellar radiation. However, the scattered light in the shadow region makes a tangible contribution to the disk surface brightness. Where, according to Figs. 3-5, the illumination by the direction radiation is close to zero, the disk surface brightness is nonzero due to the scattered light.

We calculated the disk illumination in the single scattering approximation for several models. Two of them are presented in Fig. 8. Analysis of the calculated models showed that the scattered light reduces the depth of the shadow zone only slightly in the case of small disk deformation (at small α). However, at $\alpha = 30^\circ$ the contribution from the scattered light in the shadow zone is more significant. As can be seen from Figs. 8 and 9, a bright spot emerges in the shadow zone in the inner CB disk. It appears, because the inner CB disk is strongly deformed and has a significant thickness at large angles α. Therefore, the scattered light from the perturbed region on the CB disk illuminates the outer part of its surface at a less acute angle than in the models with a lower α. As a result, in the models with strong disk deformation, the scattered light makes a tangible contribution to the illumination of the shadow zone.

Orbital Motion of the Companion and the Disk Illumination

The changes in disk illumination conditions with orbital phase are of special interest. Calculations showed that these changes occur by no means in the same way as, for example, in the model of a spotted star, where the regions of maximum and minimum illumination on the disk move azimuthally, following the stellar rotation[2] (Wood and Whitney 1998). In our case, as a result of the companion's orbital motion, the bright and dark regions execute small synchronous oscillations on the disk surface, with their shape changing only slightly. This is clearly seen from Fig. 10, which shows two disk models. The companion is at an orbital phase of 90°, in one model and at the opposite end of the orbit, at a phase of 270°, in the other model. We see that the boundary between the bright and dark zones in these two limiting situations changed only slightly. The position angle of the line separating these two regions changes with orbital phase, though within a narrow range (Fig. 11).

Asymmetry of Disks During Coronagraphic Observations

As has been pointed out in the Introduction, the method of coronagraphy, whereby the central star (along with the central region on the disk) is covered, is commonly used in the observations of circumstellar disks. We modeled this situation. Figure 12 shows two disk illumination distributions in the same model. In one of them, the central region of the system is covered by an opaque shield. The shield size relative to the disk size was chosen in such a way that it roughly corresponded to the conditions of Hubble Space Telescope observations of the circumstellar disk around one of the nearest Herbig Ae stars, HD 163296 (see Wisniewski et al. 2008). We see that, in this case, the shadow zone is covered almost completely by the artificial shield. Consequently, the coronagraphic method of imaging widely used in studying circumstellar disks can hide valuable information about the existence of an asymmetry on the disk caused by a low-mass companion from the observer.

It should be noted that in close binary systems like those we consider here with an orbital radius of the order of several AU, the dust in the perturbed region of the CB disk near its inner boundary makes a major contribution to the circumstellar extinction. Other potentially important extinction sources include the circumstellar disk surrounding the central stars and the gas flows in the inner region of the system. In the implementation of the SPH method (with a constant smoothing length) we used, this region is modeled rather roughly. Since this region has small sizes in close binary systems like those considered here, its contribution to the extinction is negligible. In wider pairs, the inner region of the system can contain much dust, and more accurate methods should be used for its calculations (Hanawa et al. 2010; Fateeva et al.

[2]The shadow region created by a dusty disk wind from the secondary component in the models by Tambovtseva et al. (2006) moves over the disk in the same way.

2011; Sytov et al. 2011; de Val-Borro et al. 2011).

CONCLUSIONS

Our calculations show that the perturbations in the circumstellar disk of a young star induced by the orbital motion of a low-mass companion whose orbit is inclined to the disk plane can cause a noticeable asymmetry in the disk illumination. It differs fundamentally in properties from what is given by the previously considered models. For example, in the models of disks with anisotropic scattering of stellar radiation by dust grains, a disk asymmetry is possible only when the disk is inclined to the plane of the sky (Augereau et al. 1999). During face-on observations, such a disk will be azimuthally uniform. In contrast, in our case, an asymmetry in the disk illumination exists at any disk inclination and is best seen during face-on observations.

In contrast to the models in which the moving bright and dark regions on the disk follow the rotation of a spotted star (Wood and Whitney 1998) or the motion of a companion that is the source of a disk wind (Tambovtseva et al. 2006), the orbital motion of the companion in our model *does not cause any synchronous motion of the shadow on the disk but leads only to small oscillations of the bright and dark regions.*. To a first approximation, the boundary between them retains its location in projection onto the plane of the sky. In this case, the line separating the illuminated region and the shadow zone, *coincide with the line of nodes*. The position angle of this line measured from the line of nodes is 40-60° (depending on the model parameters).

The amplitude of the perturbations in the disk induced by the orbital motion of the companion, along with the parameters of the bright and dark regions on the disk, depend on the component mass ratio, viscosity, and orbital inclination. Other things being equal, the smaller these parameters, the smaller the shadow zone on the disk. The minimum mass of the companion at which the asymmetry in the disk illumination is still noticeable in our calculations is about six Jupiter masses (Fig. 6).

Allowance for the influence of scattered light showed that it reduces the depth of the shadow on the disk without changing the asymmetry in the disk illumination. The case where the companion's orbit is highly inclined to the disk plane (Fig. 8) constitutes an exception. In this case, the scattered radiation forms a bright spot in the shadow region due to strong deformation of the inner CB disk. This effect was obtained in the single-scattering approximation and deserves a more detailed study by solving the 3D radiative transfer problem.

The degree of asymmetry in the illuminated region on the disk is maximal in the central part of the disk with a radius of 20-30 orbital radii and decreases with increasing distance from the center. During coronagraphic observations, this region is covered by a mask (an artificial moon) covering the star. We expect a big breakthrough in studying the asymmetry of circumstellar disk images once the ALMA interferometer has been put into operation. It will operate in the submillimeter wavelength range and will allow the central regions of protoplanetary disks to be seen without any distortions.

This work was supported by the Basic Research Program of the Presidium of the Russian Academy of Sciences P21 of the Presidium of the Russian Academy of Sciences, grant NSh 1625.2012.2 Federal Targeted Program Science and Science Education for Innovation in Russia 2012-2013.

REFERENCES

1. P. Artymowicz and S. H. Lubow, Astrophys. J. **467**, L77 (1996).
2. J. C. Augereau, A. M. Lagrange, D. Mouillet, et al., Astron. Astrophys. **348**, 557 (1999).
3. M. R. Bate, G. Lodato, and J. E. Pringle, Mon. Not. R. Astron. Soc., **401**, 1505 (2010).
4. D. J. A. Brown, A. Collier Cameron, D. R. Anderson, et al.,Mon. Not. R. Astron. Soc. Tmp. **292** (2012)
5. C. J. Burrows, J. E. Krist, K. R. Stapelfeldt, and WFPC2 Investigation Definition Team, Bull. Am. Astron. Soc. **27**, 1329 (1995).
6. S. J. Burrows, K. R. Stapelfeldt, A. M. Watson, et al., Astrophys. J. **473**, 437 (1996).
7. E. Chapillon, S. Guilloteau, A. Dutrey, et al., Astron. Astrophys. **488**, 565 (2008).
8. G. Chauvin, A.-M. Lagrange, H. Beust, et al., arXiv1202.2655C (2012).
9. M. Clampin, J. E. Krist, D. R. Ardila, et al., Astron. J. **126**, 385 (2003).
10. M. Cohen, Mon. Not. R. Astron. Soc. **173**, 279 (1975).
11. T. V. Demidova, V. P. Grinin, and N. Ya. Sotnikova, Astron. Lett. **36**, 498 (2010).
12. T. V. Demidova, N. Ya. Sotnikova, and V. P. Grinin, Astron. Lett. **36**, 422 (2010).
13. J. A. Eisner, B. F. Lane, L. A. Hillenbrand, et al., Astrophys. J. **613**, 1049 (2004).
14. A. M. Fateeva, D. V. Bisikalo, P. V. Kaygorodov, et al., Astrophys. Space Sci. **335**, 125 (2011).
15. S. A. Grady, D. Devine, B. Woodgate, et al., Astrophys. J. **544**, 895 (2000).
16. V. P. Grinin, N. N. Kiselev, G. P. Chernova, et al., Astrophys. Space Sci. **186**, 283 (1991).
17. V. P. Grinin, T. V. Demidova, and N. Ya. Sotnikova, Astron. Lett. **36**, 808 (2010).
18. T. Hanawa, Y. Ochi, and K. Ando, Astrophys. J. **708**, 485 (2010).
19. G. Hébrard, F. Bouchy, F. Pont, et al., in Transiting Planets, Ed. by F. Pont, D. Sasselov, and M. J. Holman (Cambridge: Cambridge Univ. Press, 2009), p. 508.
20. P. V. Kaigorodov, D. V. Bisikalo, A. M. Fateeva, et al., Astron. Rep. **54**, 1078 (2010).
21. S. J. Kenyon and L. Hartmann, Astrophys. J. **323**, 714 (1987).
22. J. E. Krist, K. R. Stapelfeldt, F. Ménard, et al., Astrophys. J. **538**, 793 (2000).
23. M.-A. Lagrange, D. Gratadour, G. Chauvin, et al., Astron. Astrophys. **493**, L21 (2009).
24. L. D. Larwood and J. C. P. Papaloizou, Mon. Not. R. Astron. Soc. **285**, 288 (1997).
25. M. J. McCaughrean and C. R. O'Dell, Astron. J. **111**, 1977 (1996).
26. M. J. McCaughrean, K. R. Stapelfeldt, and L. M. Close, in Protostars and Protoplanets IV, Ed. by V. Mannings, A. P. Boss, and S. S. Russell (Univ. of Arizona Press, Tucson, 2000), p. 485.
27. V. E. Mendoza, Astrophys. J. **143**, 1010 (1966).
28. D. Mouillet, J. D. Larwood, J. C. B. Papaloizou, et al., Mon. Not. R. Astron. Soc. 292, **896** (1997).
29. N. Narita, T. Hirano, B. Sato, et al., Publ. Astron. Soc. Jpn. **63**, 67 (2011).
30. A. Natta and B. Whitney, Astron. Astrophys. **364**, 633 (2000).
31. A. Natta, V. P. Grinin, and V. Mannings, in Protostars and Planets IV, Ed. by V. Mannings, A. P. Boss, and S. S. Russell (Tucson: Univ. of Arizona Press, 2000), p. 559.
32. F. Pont, M. Endl, and W. D. Cochran, Mon. Not. R. Astron. Soc. **402**, L1 (2010).
33. A. N. Rostopchina, Astron. Rep. **43**, 113 (1999).
34. N. Ya. Sotnikova, Astrofizika **39**, 259 (1996).
35. N. Ya. Sotnikova and V. P. Grinin, Astron. Lett. **33**, 594 (2007).
36. K. R. Stapelfeldt, J. E. Krist, F. Ménard, et al., Astrophys. J. **502**, L65 (1998).
37. A. Yu. Sytov, P. V. Kaigorodov, A. M. Fateeva, et al., Astron. Rep. **55**, 793 (2011).
38. L. V. Tambovtseva, V. P. Grinin, and G. Weigelt, Astron. Astrophys. **448**, 633 (2006).
39. M. de Val-Borro, G. F. Gahm, H. C. Stempels, et al., Mon. Not. R. Astron. Soc. **413**, 2679 (2011).
40. F. J. Vrba, A. E. Rydgren, P. F. Chugainov, et al., Astrophys. J. **306**, 199 (1986).
41. J. Winn, J. A. Johnson, D. Fabrycky, et al., Astrophys. J. **700**, 302 (2009a).
42. J. Winn, A. W. Howard, J. A. Johnson, et al., Astrophys. J. **703**, 2091 (2009b).
43. J. P. Wisniewski, M. Clampin, C. A. Grady, et al., Astrophys. J. **682**, 548 (2008).
44. K. Wood and B. Whitney, Astrophys. J. Lett. **506**, L43 (1998).

Translated by V. Astakhov

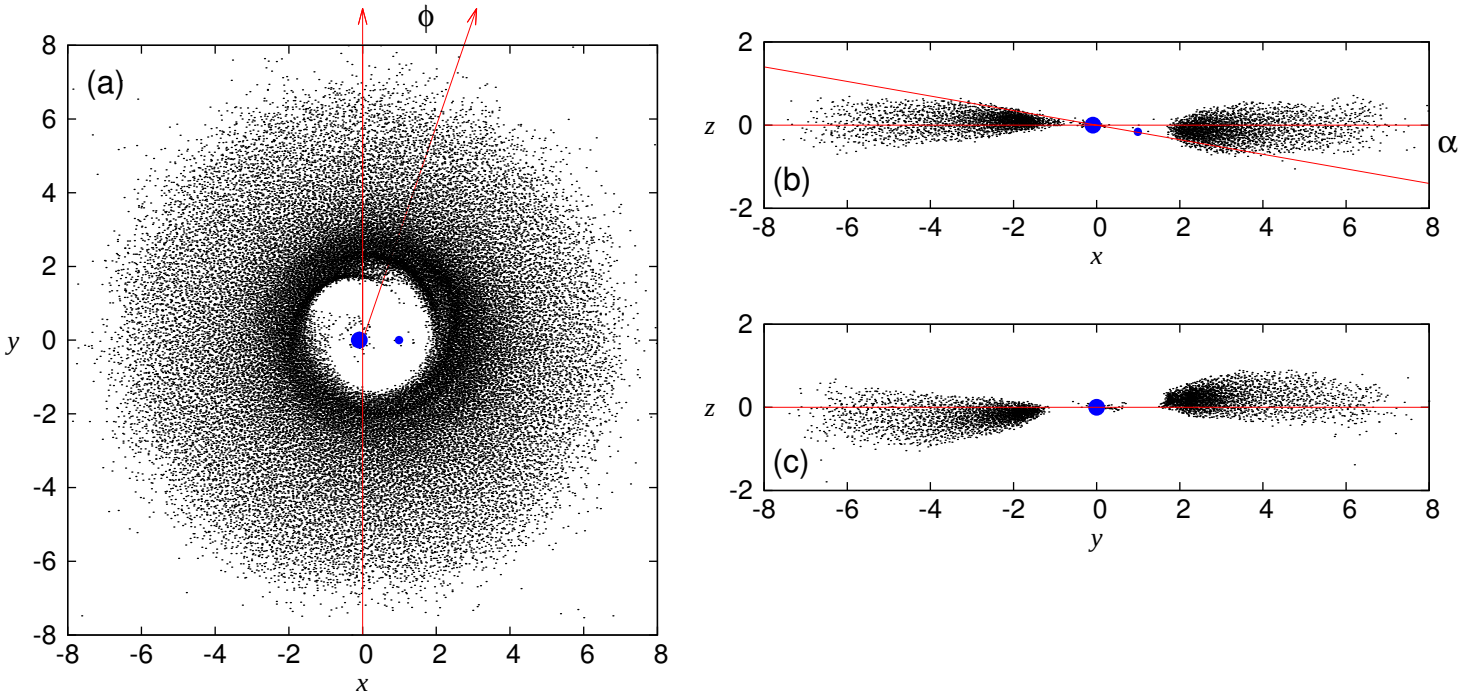

Figure 1: Distribution of matter in the disk after 30 rotations of the system: (a) face-on view, (b) and (c) disk sections along the y and x axes; here, α is the angle between the orbital plane of the binary system and the CB disk plane at the initial instant of time. The distances are in units of the binary's semimajor axis. The model parameters are: the component mass ratio $q = 0.1$, the viscosity parameter $c = 0.05$ and $\alpha = 10°$. The angle ϕ is measured from the y axis (coincident with the line of nodes) in the direction of the companion's rotation.

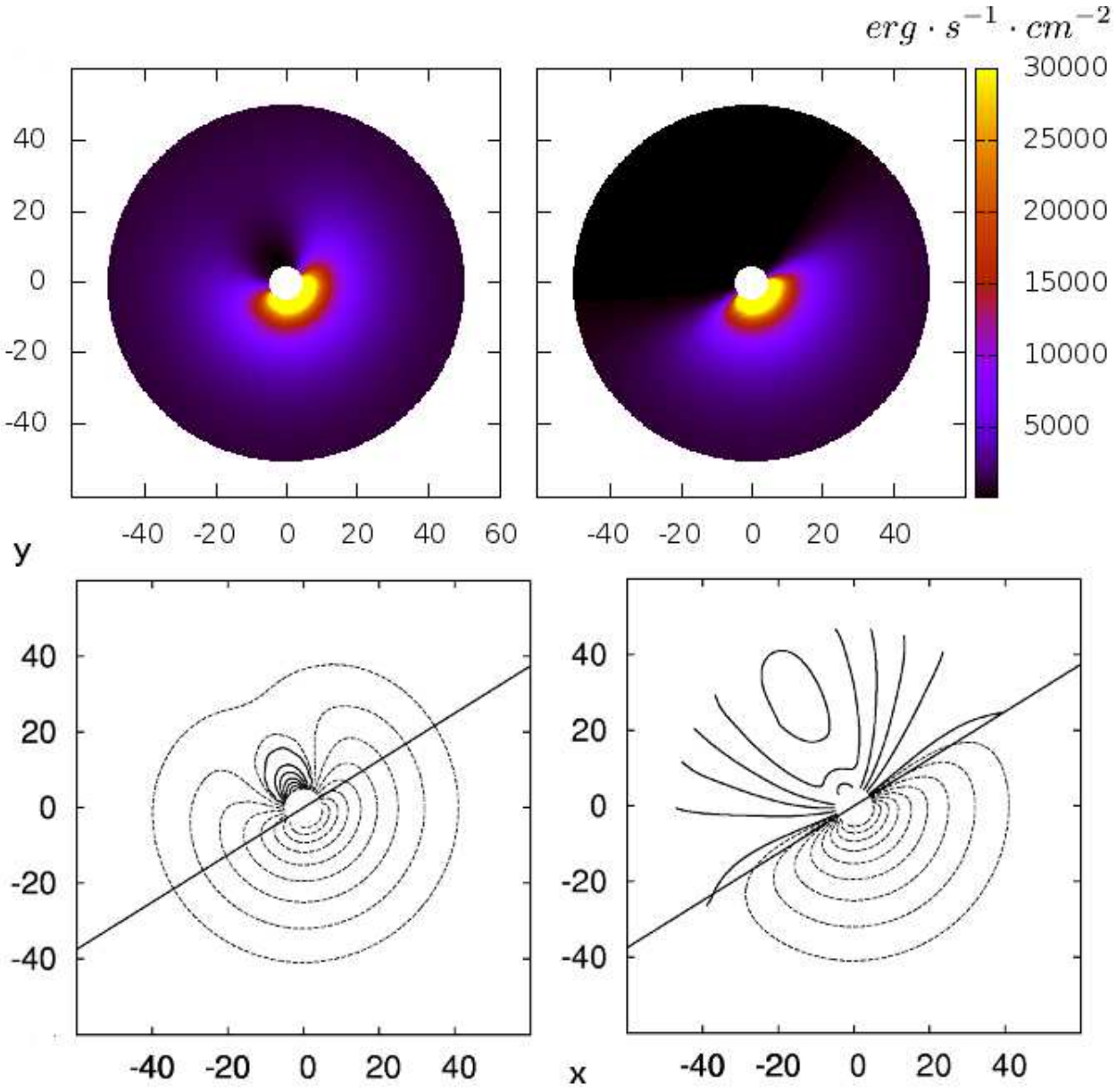

Figure 2: Top: illumination of the outer part of the CB disk by the binary's primary component for two models differing by the orbital inclination of the companion to the CB disk plane. The model parameters are: $q = 0.1$, $c = 0.05$, $\alpha = 10°$ (left) and $\alpha = 30°$. (right). The readings along the x and y axes are in units of the binary's semimajor axis; the color scale of illumination is in erg/(s×cm^2). Bottom: the same in the form of isolines; the straight line corresponds to the line separating the bright and dark (shadow) regions. The dotted lines in the lower graphs indicate the regions where the illumination is greater than that of the outer disk at a distance of $50\,a$; the solid lines indicate the regions where it is smaller than this value.

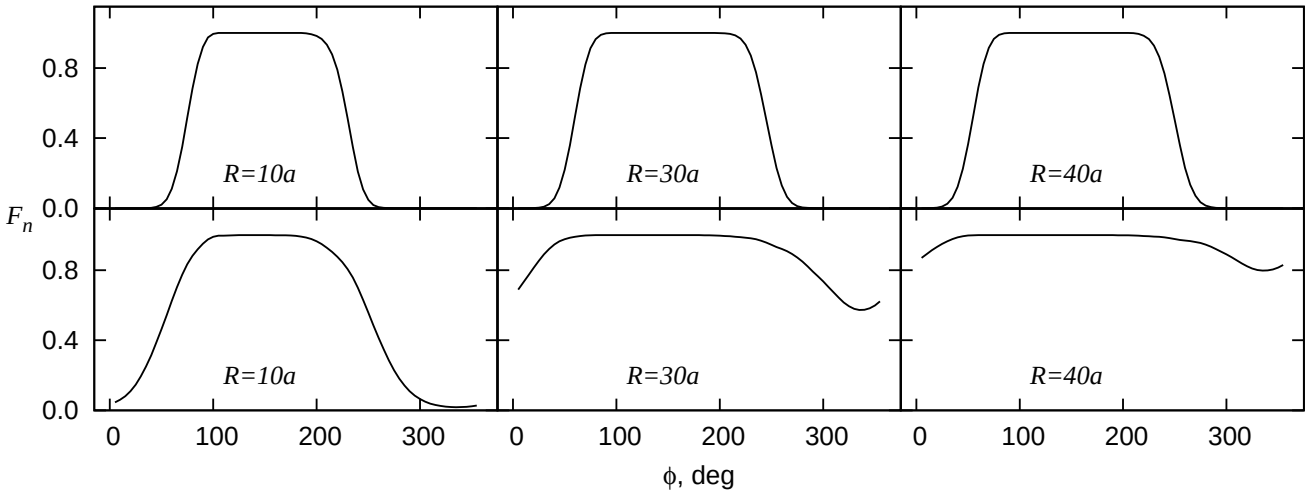

Figure 3: Normalized dependences of the disk illumination (F_n) on azimuth at three distances from the center (for the same models as in Fig. 2). The distance R is in units of the semimajor axis. $\alpha = 30°$ (top) and $\alpha = 10°$ (bottom).

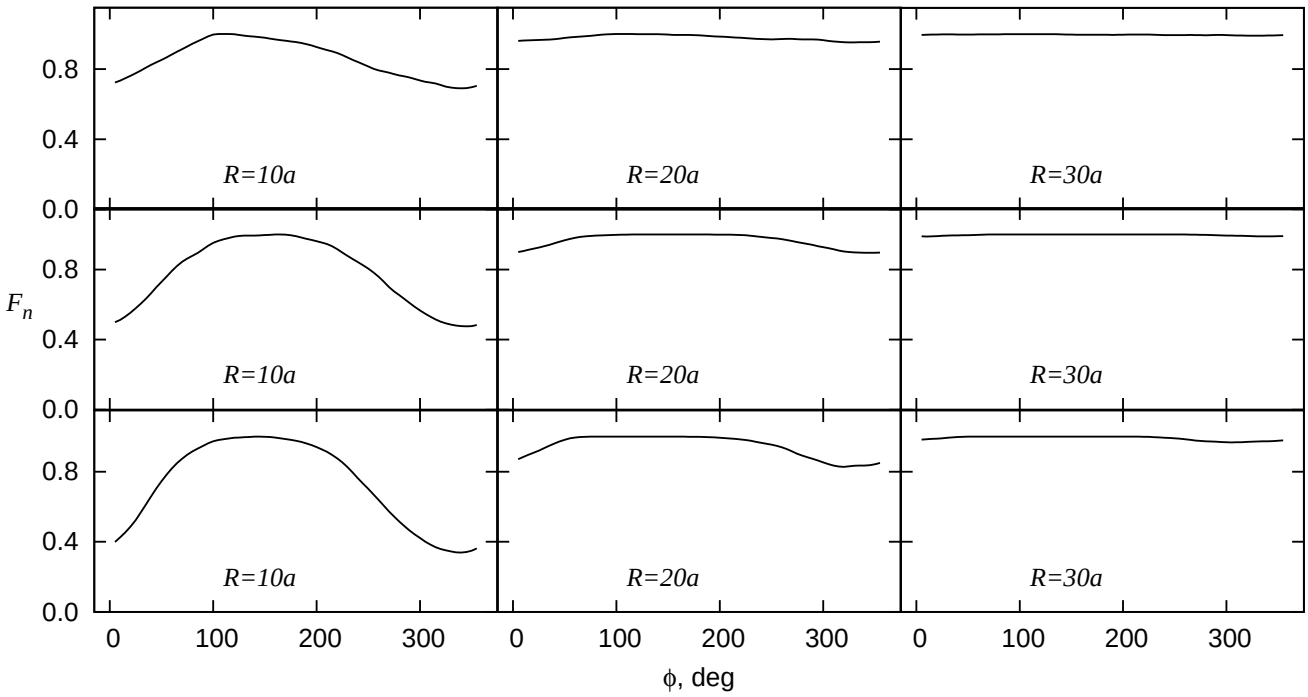

Figure 4: Same as Fig. 3 for three models differing by the companion mass: $q = 0.01$ (top), $q = 0.03$ (middle), and $q = 0.1$ (bottom). In all three models, $c = 0.05$, $\alpha = 5°$.

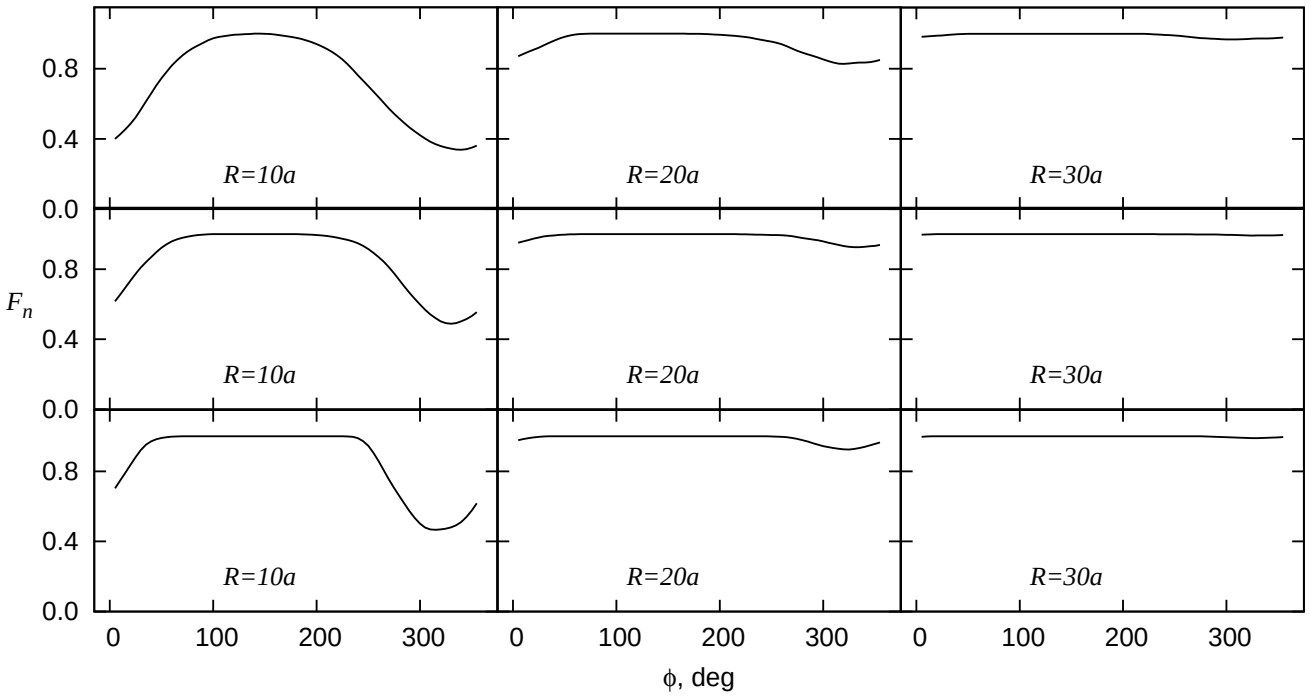

Figure 5: Same as Fig. 3 for three models differing by the viscosity: the upper, middle, and lower plots correspond to $c = 0.05$, $c = 0.04$ and $c = 0.02$, respectively. In all three models, $q = 0.1$, $\alpha = 5°$.

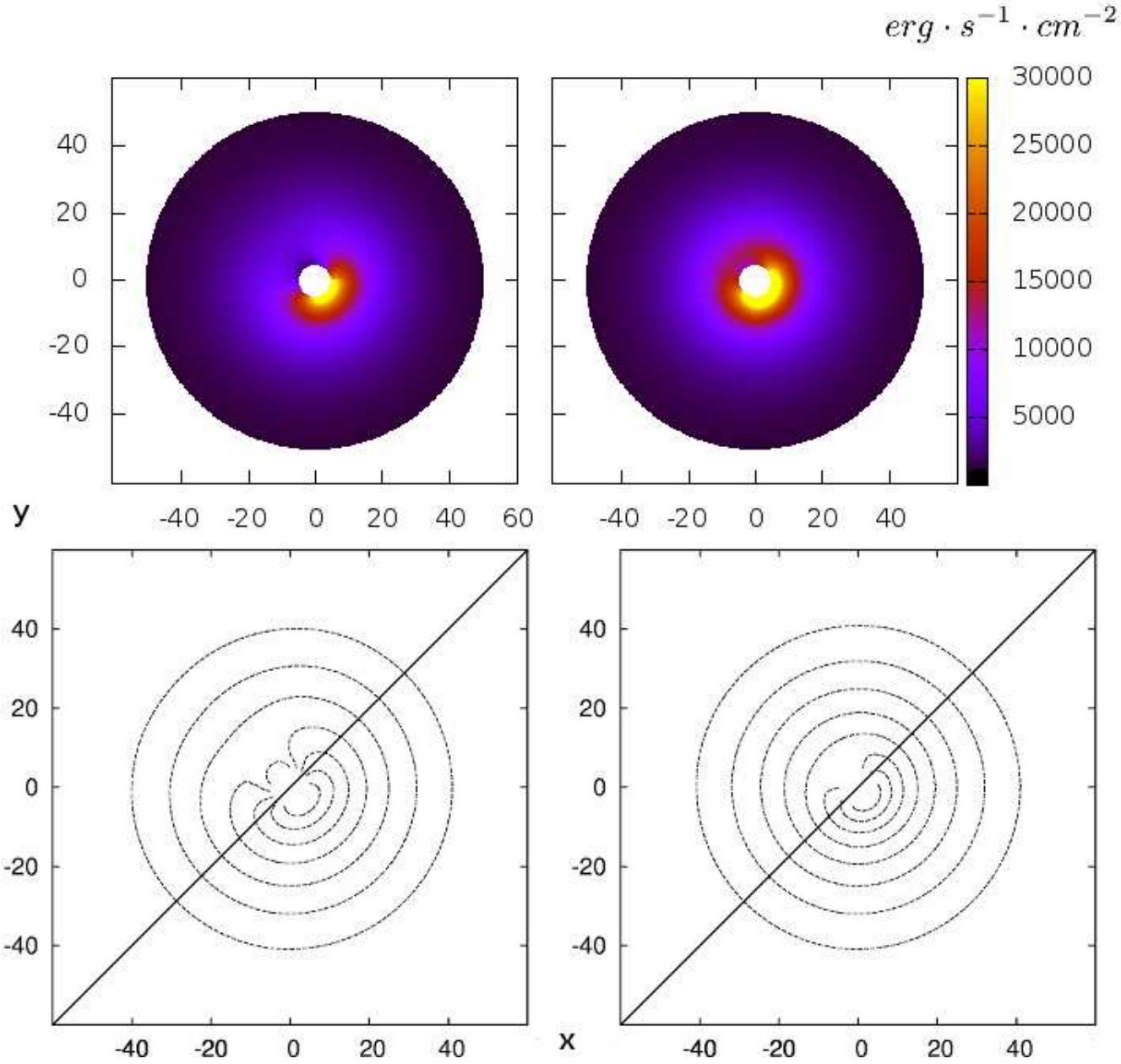

Figure 6: Small perturbations in the limiting cases. Top: the disk illumination for the models with $q = 0.003$, $c = 0.05$, $\alpha = 10°$ (left) and $q = 0.1$, $c = 0.05$, $\alpha = 3°$ (right). Bottom: the same in the form of isolines; the inclination of the line separating the dark and bright regions is $\phi_l = 46°$ (left) and $\phi_l = 44°$ (right).

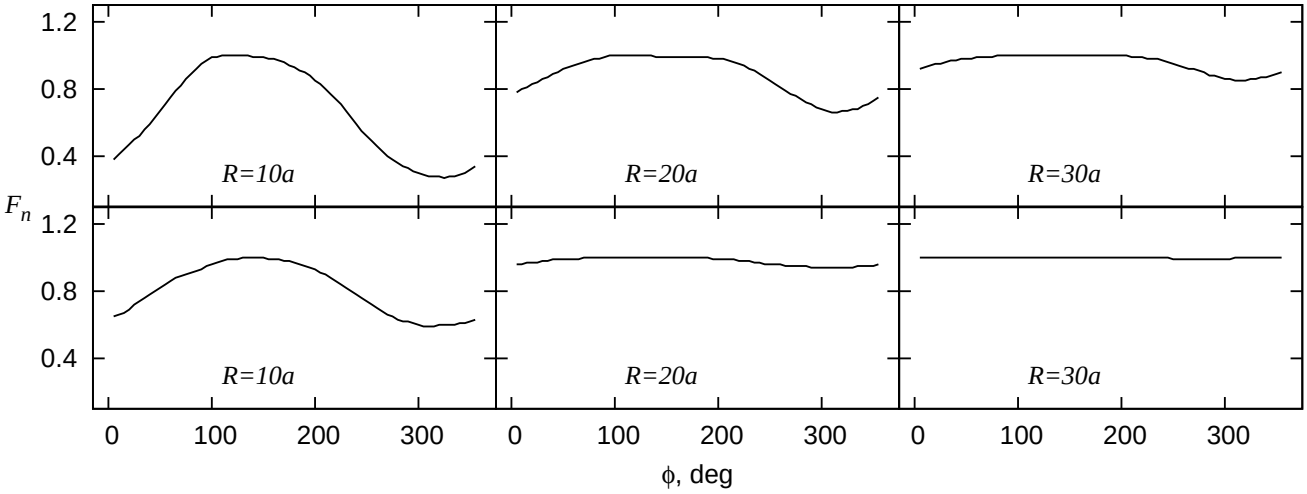

Figure 7: Same as Fig. 3 for two models with small perturbations: the upper and lower plots correspond to the models with $q = 0.003$, $c = 0.05$, $\alpha = 10^\circ$ and $q = 0.1$, $c = 0.05$, $\alpha = 3^\circ$, respectively

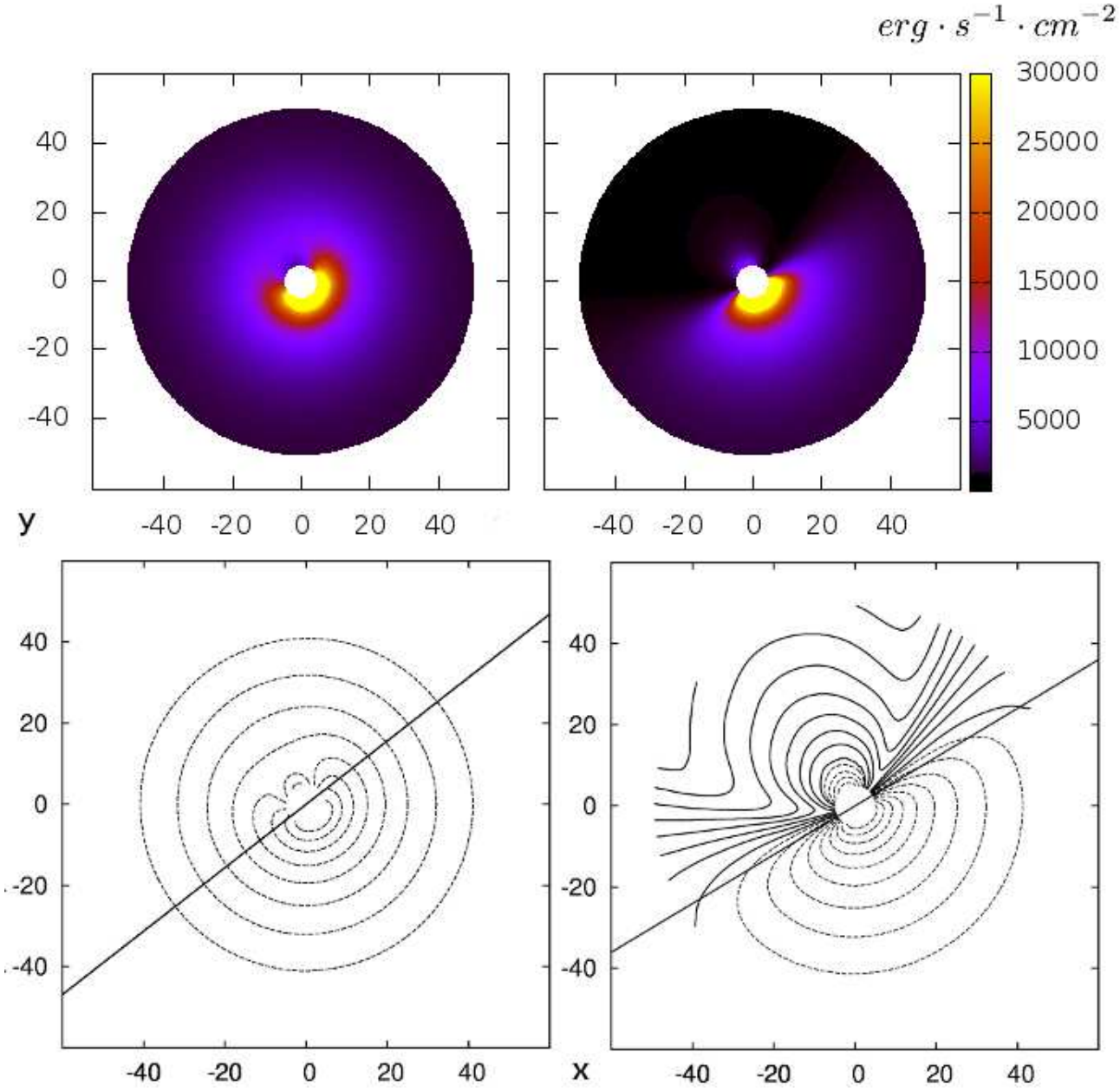

Figure 8: Top: disk illumination including the scattered light for the models with $q = 0.1$, $c = 0.05$, $\alpha = 5°$ (left) and $\alpha = 30°$. (right). Bottom: the same in the form of isolines; the inclination of the line separating the dark and bright regions is $\phi_l = 49°$ (left) and $\phi_l = 59°$ (right).

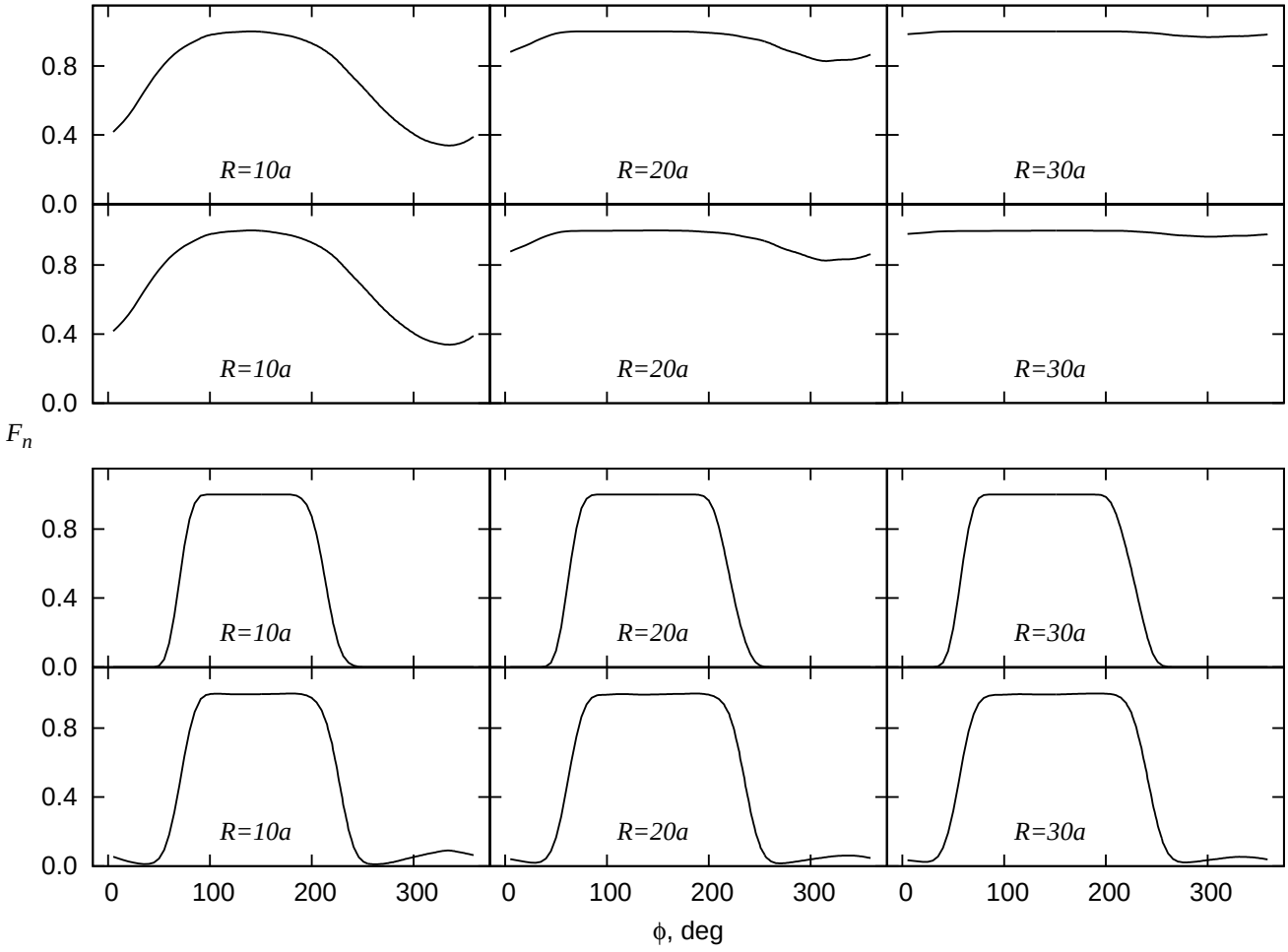

Figure 9: Same as Fig. 3 for the models with and without the scattered radiation. The model parameters are: $q = 0.1$, $c = 0.05$, $\alpha = 5^\circ$ (the upper pair of plots) and $\alpha = 30^\circ$. (the lower pair of plots). The upper and lower plots in each pair show the dependence F_n without and with the scattered light, respectively.

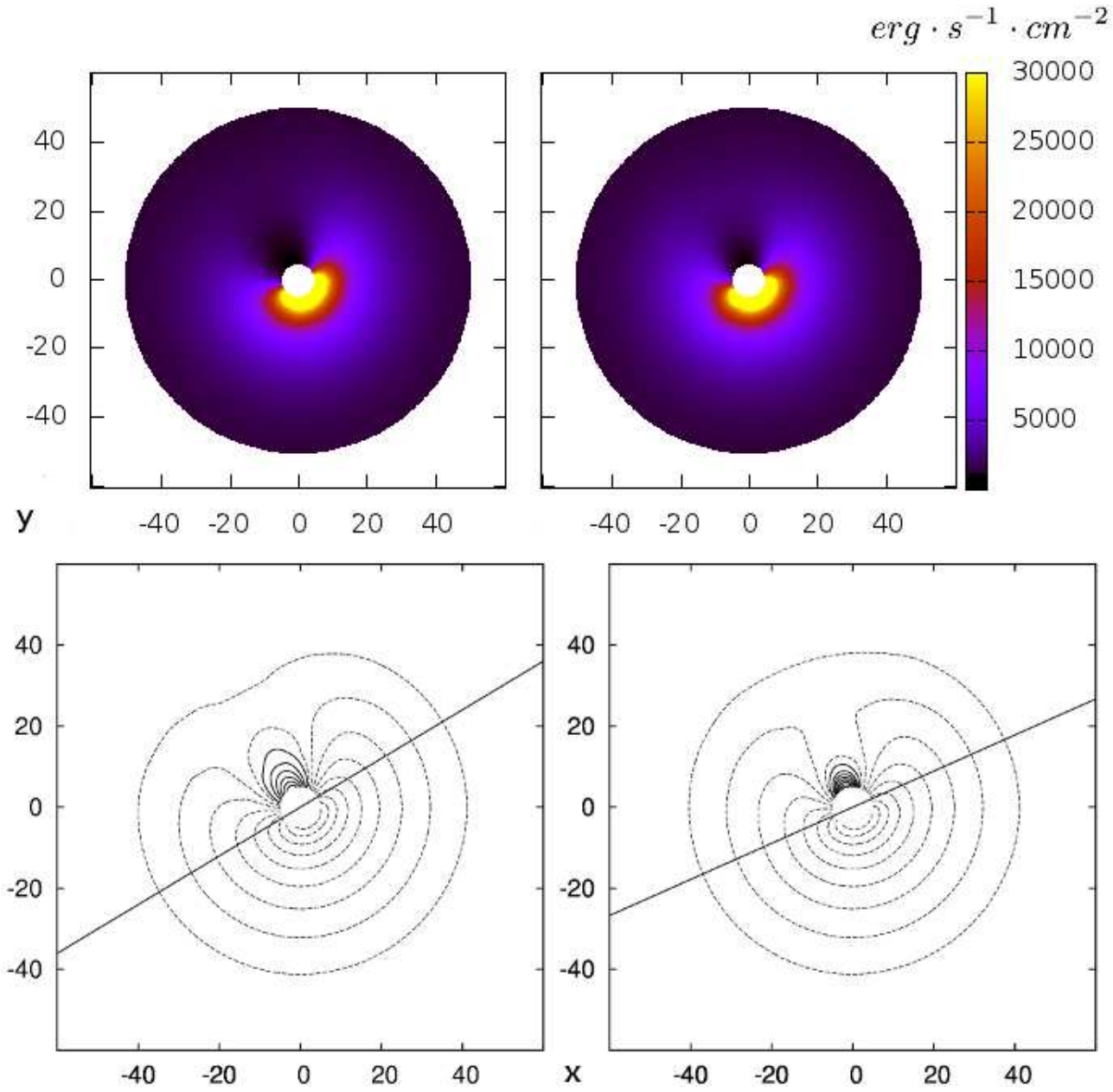

Figure 10: Illumination of the outer CB disk (with the scattered light) for two positions of the secondary components in its orbit. Left: the companion is at $\phi = 90°$ (under the disk), the inclination of the separating line is $\phi_l = 58°$; right: $\phi = 270°$ (the companion is above the disk), $\phi_l = 71°$. The model parameters are $q = 0.1$, $c = 0.05$ end $\alpha = 10°$.

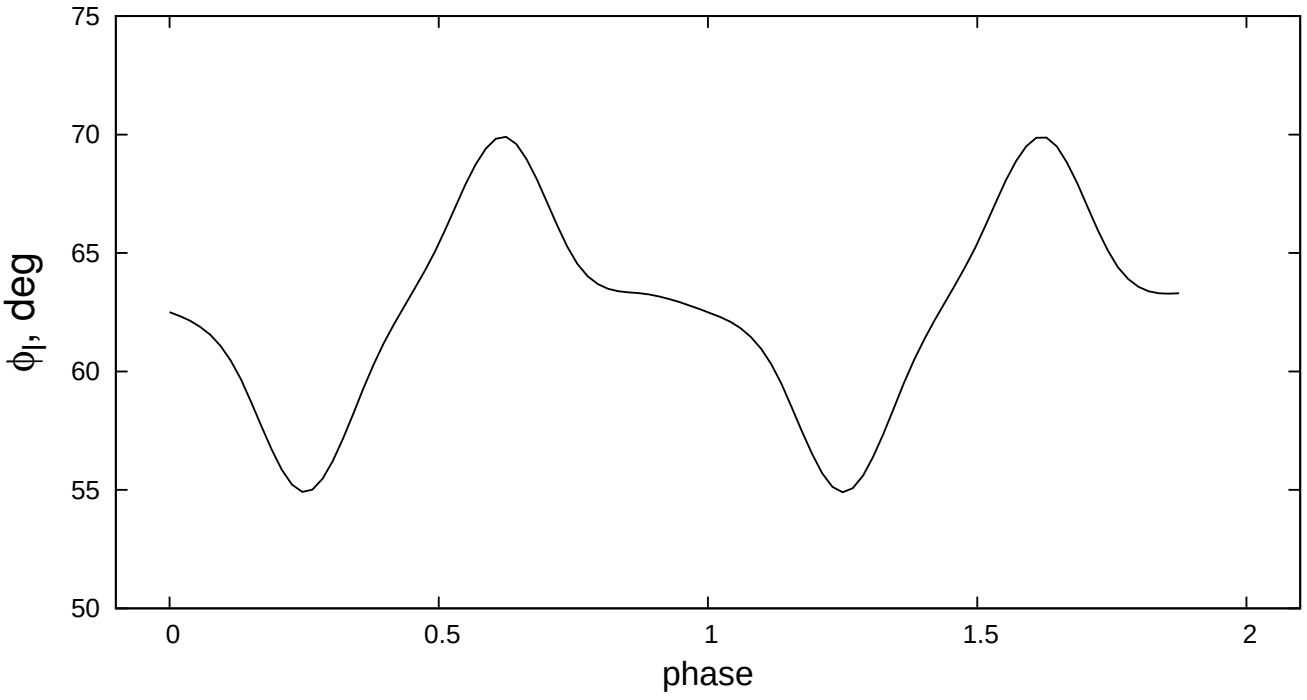

Figure 11: Inclination (ϕ_l) of the line separating the bright and dark regions versus orbital phase. The model parameters are $q = 0.1$, $c = 0.05$ and $\alpha = 10^\circ$. Phase 0 corresponds to the position of the component at $\phi = 0^\circ$.

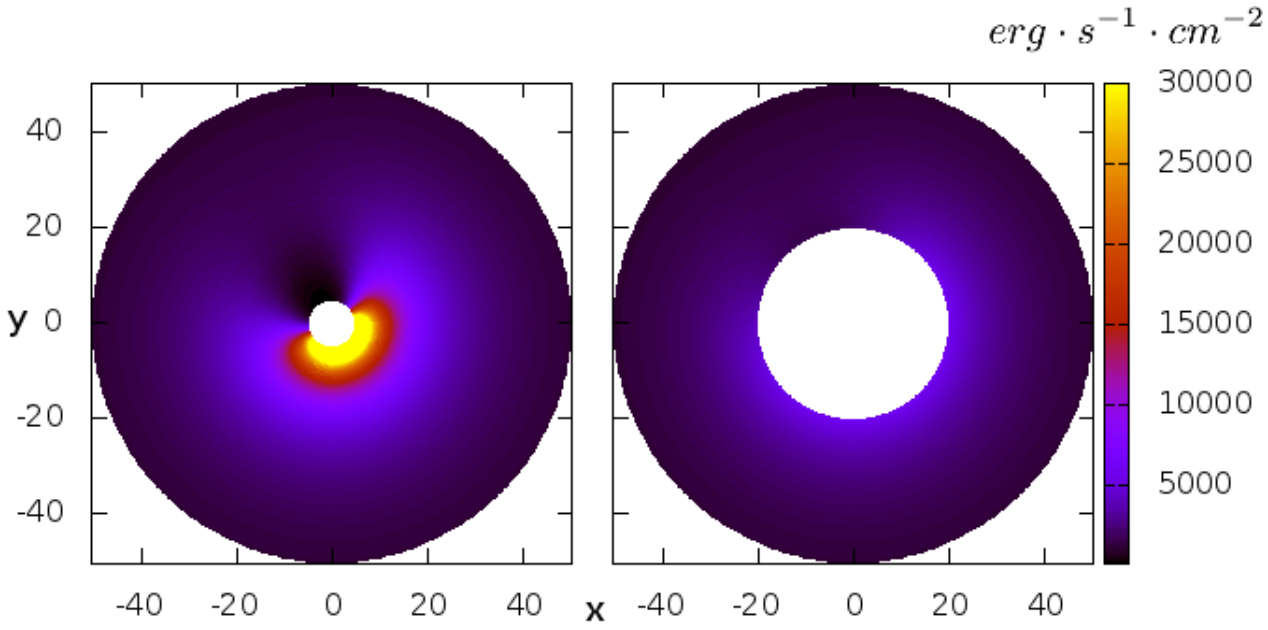

Figure 12: Illumination of the outer CB disk. The model parameters are $q = 0.1$, $c = 0.05$ and $\alpha = 10°$. The entire disk and only its outer region (the inner part with a size $R < 20a$ is covered by an opaque shield) are shown on the left and the right, respectively.